AD-A110 433 CHICAGO UNIV IL JAMES FRANCK INST F/G 20/2
NUCLEAR TRANSMUTATION DOPING OF GAAS.(U)
SEP 81 H FRITZSCHE AFOSR-80-0231
UNCLASSIFIED AFOSR-TR-82-0024 NL

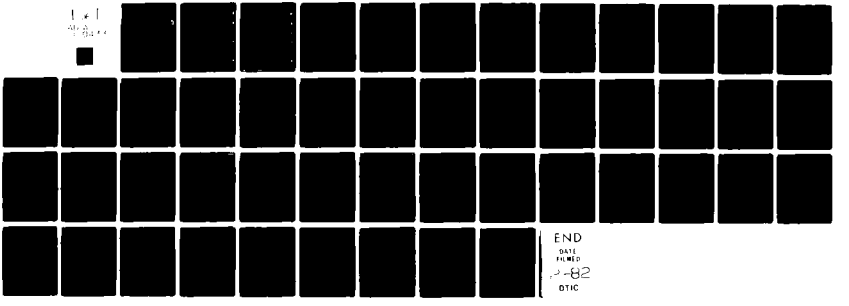

END
DATE FILMED
2-82
DTIC

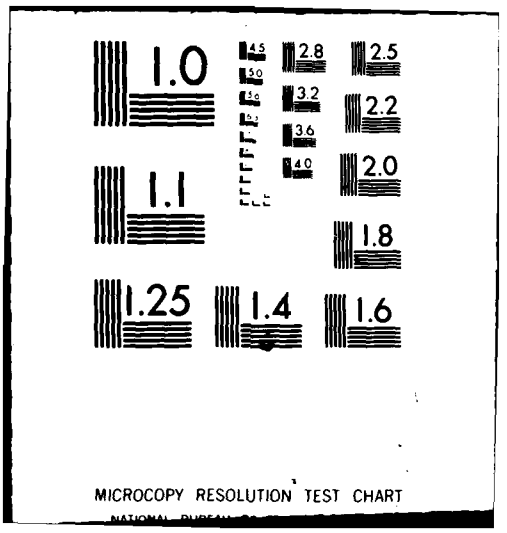
1.0
1.1
1.25
1.4
1.6
1.8
2.0
2.2
2.5
2.8
3.2
3.6
4.0
4.5
5.0
MICROCOPY RESOLUTION TEST CHART

LEVEL II 19



# NUCLEAR TRANSMUTATION DOPING OF GaAs

FINAL TECHNICAL REPORT

Grant No. AFOSR-80-0231

for the period

June 1, 1980 to June 30, 1981

submitted to the

AIR FORCE OFFICE OF SCIENTIFIC RESEARCH



by

THE UNIVERSITY OF CHICAGO
DIVISION OF THE PHYSICAL SCIENCES
THE JAMES FRANCK INSTITUTE
5640 South Ellis Avenue
Chicago, Illinois 60637



Prepared by

H. FRITZSCHE,
Principal Investigator
Tel. (312) 753-8221

September 1981

Unclassified

SECURITY CLASSIFICATION OF THIS PAGE (When Data Entered)

| REPORT DOCUMENTATION PAGE | | READ INSTRUCTIONS BEFORE COMPLETING FORM |
|---|---|---|
| 1. REPORT NUMBER AFOSR-TR- 82-0024 | 2. GOVT ACCESSION NO. AD A110 | 3. RECIPIENT'S CATALOG NUMBER 433 |
| 4. TITLE (and Subtitle) Nuclear Transmutation Doping of GaAs | | 5. TYPE OF REPORT & PERIOD COVERED FINAL, 1 June 80-30 Jun 81 |
| | | 6. PERFORMING ORG. REPORT NUMBER |
| 7. AUTHOR(s) Hans Fritzsche | | 8. CONTRACT OR GRANT NUMBER(s) AFOSR - 80-0231 |
| 9. PERFORMING ORGANIZATION NAME AND ADDRESS University of Chicago James Franck Institute Chicago, ILL. 60637 | | 10. PROGRAM ELEMENT, PROJECT, TASK AREA & WORK UNIT NUMBERS 61102F 2306/B1 |
| 11. CONTROLLING OFFICE NAME AND ADDRESS AFOSR/NE Bolling AFB, Washington, D.C. 20332 | | 12. REPORT DATE SEPT 81 |
| | | 13. NUMBER OF PAGES 46 |
| 14. MONITORING AGENCY NAME & ADDRESS(if different from Controlling Office) | | 15. SECURITY CLASS. (of this report) UNCLASSIFIED |
| | | 15a. DECLASSIFICATION/DOWNGRADING SCHEDULE |

16. DISTRIBUTION STATEMENT (of this Report)

Approved for public release; distribution unlimited.

17. DISTRIBUTION STATEMENT (of the abstract entered in Block 20, if different from Report)

18. SUPPLEMENTARY NOTES

10

19. KEY WORDS (Continue on reverse side if necessary and identify by block number)

GaAs, nuclear transmutation doping, magnetoresistance

20. ABSTRACT (Continue on reverse side if necessary and identify by block number)

Shallow donors have been introduced into GaAs crystals by irradiation with thermal neutrons and subsequent nuclear transmutation. Good agreement was found between the measured concentrations of added donors and the values expected from the neutron capture cross sections and the neutron fluences used. This doping -

DD FORM 1 JAN 73 1473 EDITION OF 1 NOV 65 IS OBSOLETE

Unclassified

SECURITY CLASSIFICATION OF THIS PAGE (When Data Entered)

Continued - Gerald Witt, 2306/B1

method is approximately 1000 times more efficient in GaAs than in Si because of the higher abundances and neutron capture cross sections of the transmutable isotopes in GaAs. In epitaxially grown GaAs of high purity, the recoil and radiation damage associated with transmutation doping can be removed by annealing at about 600°C which is below the critical temperature for As effusion. The electronic transport properties of transmutation doped GaAs samples were studied between 1.4 and 450K of concentrations both above and below the metal-nonmetal transition. We found that transmutation doping is a convenient method for introducing a desired concentration of shallow donors into GaAs crystals for modifying their electronic properties.

TABLE OF CONTENTS

# I. ABSTRACT OF RESEARCH GOAL

GaAs crystals containing well-controlled impurity concentrations are in great demand for high frequency and high speed GaAs devices. The quality and control of impurities in GaAs material is much less advanced than in elemental semiconductors such as Si. This is partly because substitutional dopants can occupy either Ga sites or As sites and they tend to associate with other defects. The method of nuclear transmutation doping will be applied to preparing homogeneous and well-controlled GaAs material. The doping characteristics, the annealing requirements for removal of radiation defects, and the resulting electrical properties of transmutation-doped GaAs will be examined.

## II. SUMMARY OF RESULTS AND ACCOMPLISHMENTS

Shallow donors have been introduced into GaAs crystals by irradiation with thermal neutrons and subsequent nuclear transmutation. Good agreement was found between the measured concentrations of added donors and the values expected from the neutron capture cross sections and the neutron fluences used. This doping method is approximately 1000 times more efficient in GaAs than in Si because of the higher abundances and neutron capture cross sections of the transmutable isotopes in GaAs. In epitaxially grown GaAs of high purity the recoil and radiation damage associated with transmutation doping can be removed by annealing at about 600°C which is below the critical temperature for As effusion. The electronic transport properties of transmutation doped GaAs samples were studied between 1.4 and 450K of concentrations both above and below the metal-nonmetal transition. We found that transmutation doping is a convenient method for introducing a desired concentration of shallow donors into GaAs crystals for modifying their electronic properties.

## III. INTRODUCTION

Superior GaAs material is in great demand for high frequency and high speed GaAs devices such as Impatt diodes, Gunn diodes, field effect transistors and avalanche photodiodes. The quality and control of impurities in GaAs material is much less advanced than in elemental semiconductors such as Si. This is partly because substitutional dopants can occupy either Ga sites or As sites and they tend to associate and cluster. We have used a new method for preparing homogeneous and well controlled GaAs material, namely The Neutron Transmutation Doping (NTD). This method was used for the first time by Cleland, Lark. Horovitz and Pigg[1], thirty years ago. They showed that it is a convenient and highly reproducible method for introducing a homogeneous distribution of dopants into certain semiconductors. This work was continued by Fritzsche et al.[2], Cuevas[3], and others[4], who made a detailed investigation of the electronic transport properties of transmutation doped Ge. This method was applied to Te by Kuehnel et al.[5], to InSb by Kuchar et al.[6], and is now widely used in the manufacture of Si devices.

Besides a brief study by Mirianashvili et al.[7], no detailed investigation of transmutation doping has been carried out on GaAs. This is quite surprising in view of the importance of GaAs as device material and the difficulties encountered with regard to impurity and vacancy complexes and the question whether Ge or other impurities are on Ga or As sites.

In the second section of this paper the theory of NTD in GaAs is discussed; section IIA is on NTD processes and the number of dopants and it is followed by a section on damages due to the recoils of $\gamma$-and $\beta$- particles produced by the NTD processes. In section III the experimental details are discussed. Undoped (not intentionally doped), Cr-doped (semi-insulating) melt-grown GaAs crystals as well as one epitaxially grown (pure) GaAs crystal were exposed to various fluxes

of thermal neutrons. The data of Hall effect R and resistivity $\rho$ measurement between 450 and 1.4K for undoped and Cr-doped samples are given in section IVA. In section IVB a two band model which is used to estimate the compensation ratio is discussed. The R and $\rho$ data for the epitaxial sample are given in section IVC. Section IVD presents magnetoresistance measurements on all samples. The metal to nonmetal transition (M-NM) and its relation to the magnetoresistance is discussed in section V. The last section presents a summary and our conclusion. Part of the data of section IVA were reported in a previous paper.[8]

## IV. THEORY OF NTD IN GaAs

### A. NTD process and the density of dopants.

Introducing dopants into GaAs by the way of transmutation is done as follows: Thermal neutrons are captured by various nuclei in GaAs in proportion to the relative abundance of Ga and As isotopes and their capture cross section. After a neutron is captured by, for instance, an $^{75}As$ nucleus, a $^{76}As$ nucleus is formed which is in an excited state. This excited nucleus decays quickly to its ground state by emitting a photon

$$^{75}As + n \rightarrow {}^{76}As + \gamma \qquad (1)$$

This new $^{76}As$ nucleus is however not stable. It decays into a $^{76}Se$ nucleus by $\beta$-particle emission.

$$^{76}As \rightarrow {}^{76}Se + \beta^- \qquad (2)$$

All naturally occurring isotopes of Ga and As participate in transmutation doping with the following reactions:

$$^{69}Ga(n,\gamma)^{70}Ga \rightarrow {}^{70}Ge + \beta^- \qquad (21\ m)^9 \qquad (3)$$

$$^{71}Ga(n,\gamma)^{72}Ga \rightarrow {}^{72}Ge + \beta^- \qquad (14\ h)^9 \qquad (4)$$

$$^{75}As(n,\gamma)^{76}As \rightarrow {}^{76}Se + \beta^- \qquad (26\ h)^9 \qquad (5)$$

The numbers in parantheses are half lives for the β-decays. If the resultant Ge atoms are found at Ga sites and the Se atoms at As sites, one expects that all end products act as donors.

The density of transmutation donors $n_{NTD}$ due to the capture of thermal neutrons follows from

$$n_{NTD} = \Phi \sum_i n_i \sigma_c^i \qquad (6)$$

where $\Phi = \phi t$ is the thermal neutron fluence (flux X time), $n_i$ is the concentration of ith isotope and $\sigma_c^i$ is its capture cross section.

If the capture cross section increases with the inverse of the neutron velocity then one obtains

$$\sigma_c = (\sqrt{\pi}/2)\sqrt{300/T}\, \sigma_c (V_o) \qquad (7)$$

where $V_o$ = 2200 m/s is the most probable neutron velocity at 300K and T is the effective neutron temperature. Combining Eqs. (6) and (7) yields

$$n_{NTD} = (\sqrt{\pi}/2) \sqrt{300/T} \sum_i n_i \sigma_c^i (V_o) \qquad (8)$$

Up to now we have only considered thermal neutrons. The neutrons in a reactor cannot be described simply by a thermal spectrum, they have a wide energy spread $\phi$ (E) extending from 1 mev to 10 Mev, thus, in addition to thermal neutrons we should consider neutron absorption due to the resonance capture which takes place in the epithermal part of the neutron flux. Contributions from the high energy region (above the epithermal part) are however negligible since neutron capture cross sections in general decrease as 1/V. Therefore, the cross sections for higher energy neutrons are a few orders of magnitude smaller than those in the thermal region. Furthermore, the non-thermal neutron density is very small at the places in the reactor chosen for the irradiation.

Finally when all types of (n,γ) reactions are included the transmutation donor density can be expressed by

$$n_{NTD} = \Phi \sum_i n_i (A\sigma_c^i (V_o) + BI^i) \qquad (9)$$

where $B = 2X10^{-2}$ is the ratio of the epithermal to the thermal flux of neutrons per unit lethargy (the logarithmic interval of the energy), $I^i$ is the resonance integral for ith isotope and $A = (\sqrt{\pi}/2) \times (300/T)^{1/2}$. The values of $n_i, \sigma^i$ and $I^i$ for Ga and As isotopes are listed in Table 1.

From the values listed in Table I and Eq. (9) we obtain

$$n_{NTD} = \Phi\ (2.435/\sqrt{T} + 0.036) \qquad (10)$$

Unfortunately after the transmutation reactions (3)-(5) the transmuted atoms are usually not in their original positions but displaced into interstitial positions due to the recoil produced by the $\gamma$ and $\beta$ particles in the nuclear reactions. Part of this study is to see whether the transmuted atoms can be returned to their original positions and radiation damages can be healed by annealing the samples.

### B. *Damage and annealing*

After the GaAs samples have been irradiated in the reactor and the induced radioactivity has been allowed to decay, the samples are found to have very low carrier concentrations and very high resistivities. This is due to deep lying defect levels which are produced during transmutation doping. The causes for these defects are (i) fast neutron knock-on displacements, (ii) gamma recoil, (iii) beta recoil. Damages due to the fast neutrons are discussed by many authors[11] and so will not be discussed here. The recoil energies from the $\gamma$ and $\beta$ emissions are

$$E_R(\gamma) = E_\gamma{}^2/2Mc^2 \qquad (11)$$

$$E_R(\beta) = E_\beta(E_\beta + 2mc^2)/2Mc^2 \qquad (12)$$

where M is the mass of the recoiling nucleus, m is the electron rest mass and $E_\gamma$ and $E_\beta$ are the energies of $\gamma$- and $\beta$- particles, respectively.

The recoil energies due to the $\gamma$- emission cover a range of values because various decay channels are possible. Decay with the highest $\gamma$- energy $E_\gamma \approx 7.5$ Mev

occurs with low probability (1%)[12]. The most probable decay proceeds by emission of two or three photons of lower energies. Table II lists the recoil energies involving one, two, and three photons, respectively.

The range of recoil energies associated with β- decay depends on the correlation between the emitted neutrino and the β- particle. We list in Table II also the maximum $E_R(\beta_{max})$ and most probable values $E_R$ (β) of the β- recoil energy.

Since only 9eV and 10eV are required for the creation of Frenkel defects in the Ga- and in the As- sublattices of GaAs respectively[13], one finds that the number of defects due to the beta and gamma recoils as well as to fast neutron knock-on displacements is very large indeed. This agrees with our finding that the samples have a very high resistivity and very low carrier concentrations after irradiation.

For removing these damages high temperature annealing was needed: 800°C for melt grown crystals and 600°C for the epitaxial one.

## V . EXPERIMENTAL DETAILS

Undoped and Cr-doped (semi-insulating) melt-grown crystals were purchased from Laser Diode Lab. Inc. Bridge-shaped samples with three electrode arms on one side and one electrode arm on the other side having enlarged pads for current contact were ultrasonically cut from 0.1 cm thick wafers. Both undoped and Cr-doped samples were etched in $1H_2O$, 5 $H_2SO_4$, $1H_2O_2$ solution. Ohmic contacts were made by alloying small balls of Ge-Au to the samples at 450°C. The undoped crystals contained an excess electron concentration of about $3X10^{16}cm^{-3}$ with the exception of one sample which had $5x10^{16}cm^{-3}$. The Cr- doped crystals had a room temperature resistivity larger than $10^7$ ohm-cm. The epitaxially grown crystal[14] was a square platelet with dimensions 0.5x0.5x0.02 cm. This sample

contained $2.1 \times 10^{14} cm^{-3}$ donors and $5.7 \times 10^{13} cm^{-3}$ acceptors.

The samples were irradiated at the Research Reactor Facility of the University of Missouri in a thermal neutron flux of $\phi = 5 \times 10^{11}$ $n/cm^2$-sec. The actual thermal neutron temperature was about 30° higher than room temperature. The total neutron dose (fluence) was measured by rhodium wire with a maximum error of 5% in $\Phi$.

Annealing of the melt-grown samples was carried out at 800°C in an inert gas atomosphere after a pyrolytic $Si_3N_4$ encapsulation to prevent As evaporation. The epitaxial layer was annealed at 600°C for 1 hour also in an inert gas atmosphere.

## VI. RESULTS AND DISCUSSION

### A. Undoped and Cr-doped samples.

Table III lists the Hall coefficient R, resistivity $\rho$, as well as the electron density $n = 1/Re$, and the Hall mobility $\mu_H = R/\rho$ measured at 300K before and after transmutation doping for the undoped melt-grown GaAs. The unirradiated sample No. 0, is included in Table III for testing the quality of the $Si_3N_4$ encapsulation. This sample was measured before and after annealing at 800°C for 10.5 hours. It is known that As atoms evaporate at temperature higher than 650°C and produce vacancy-donor complexes[15]. These are expected to result in a reduction in n, and $\mu_H$. Instead we observe a small increase in carrier concentration and an improvement in mobility. It appears that annealing removes some low-lying acceptor states which were initially present in the material but no effects of As evaporation were observed. Since the Hall factor $r = nRe$ is larger than one for an isotropic band such as the conduction band of GaAs[16], the carrier concentrations n, given in Table III are underestimated. Measurement at 450K indicated that considering the carrier density at 300K as the excess electron

concentration would be an underestimation by less than 10% due to the carrier freeze-out. The last two rows in Table III compare the measured change in carrier concentration $\Delta n$ with that expected from Eq. (10), using the irradiation fluences $\Phi$ listed in row 5. The errors in the last row were calculated from the errors in fluences and the errors in capture cross sections. By considering the increase in carrier concentration because of the annealing alone and the underestimation due to the carrier freeze-out at 300K and due to using Hall factor r = 1, we find the close agreement between the measured and calculated values of the donor concentration introduced by transmutation doping very satisfactory. This shows that indeed most Ge atoms are on Ga sites and most Se atoms are on As sites after annealing. Intersite defects are expected to act as acceptors; the agreement between $\Delta n$ and $n_{NTD}$ indicates that fewer than 5% transmuted atoms form intersite defects. Table IV lists the values of R, $\rho$, $\mu_H$, and n measured at 300K after the irradiation and annealing for the Cr- doped melt-grown samples, in addition, $n_{NTD}$ for each sample. Annealing was carried out at 800°C for 4.5 hours.

The efficiency of transmutation doping in Cr- doped GaAs cannot be assessed by comparing the last two rows of Table IV. This is because these samples are compensated and therefore the compensation ratio $K = N_A/N_D$ must be determined before one can obtain $N_D$ from the measured $n_o = N_D - N_A$. K cannot be determined by using ordinary analysis of the temperature dependence of carrier concentration because the change in Hall coefficient and hence in carrier concentration n due to the temperature change is small (see Fig.2). In the next section we will use a two band model for estimating K. Fig. 1 and 2 show the temperature dependence of $\rho$ and R respectively for the samples listed in Table III and IV. The non-irradiated sample before annealing is denoted by (00) and after annealing by (0). The resistivity curves show two activation regimes. The larger activation energy

$E_1$ at high temperature is due to excitation of carriers into the conduction band. The smaller low temperature activation energy $E_2$ which goes to zero as the carrier concentration n reaches $3\times10^{16}cm^{-3}$, is associated with the impurity band conduction. The maximum in the Hall curves near 80K is due to the transition from band conduction to impurity conduction. This will be discussed in the next section.

B. Two band conduction.

When the impurity levels are separated in energy from the conduction band, the conduction band carriers freeze out into the impurity levels as the temperature is lowered. Since R is inversely proportional to the carrier density, we expect R to increase with decreasing temperature. Our results as well as those of other groups[17-24] on GaAs show that R does not rise indefinitely but goes through a maximum as the temperature is decreased. The same behavior has been observed in Ge[25], InSb[26], InP[24] and other semiconductors. At low temperatures the conduction process is dominated by phonon-assisted hopping of electrons among the impurity levels. The Hall maximum occurs at the temperature where band conduction and impurity conduction are of comparable magnitude. The expression for $\sigma$ and R for two band conduction are[27]

$$\sigma = e(n_c\mu_c + n_i\mu_i) \tag{13}$$

$$R = \frac{1}{e}\,(n_c\mu_c^2 + n_i\mu_i^2)/(n_c\mu_c + n_i\mu_i)^2 \tag{14}$$

where $n_c$ and $\mu_c$ are the concentration and the mobility of the carriers in the conduction band and $n_i$ and $\mu_i$ are the corresponding values of the carriers moving between the impurities.

The total electron density for n-type material in extrinsic region is

$$n_o = N_D - N_A = n_c + n_i \tag{15}$$

Now Eq. (14) can be written as

$$R = (1/n_o e)\frac{[x(b^2-1)+1]}{[x(b-1)+1]^2} \tag{16}$$

with $b = \mu_c/\mu_i$ and $x = n_c/n_o$. Since b changes slowly with temperature compared to $n_c$, R in Eq. (16) will have a maximum at $x = 1/(b+1)$. This occurs when impurity conduction is equal to the band conduction. One can obtain the value of b from Eq. (16) and the condition for the Hall maximum.

$$(R_{max}/R_{exh}) = (b+1)^2/4b \qquad (17)$$

where $R_{max}$ is the value of R at its maximum and $R_{exh} = 1/n_o e$ is the value of R in the exhaustion range where all donors are ionized. Using the value of b, obtained from Eq. (17), the exhaustion electron concentration $n_o$ and the measured Hall coefficient at a given temperature, one can calculate x from Eq. (16) and hence the electron concentration $n_c = xn_o$ at that temperature. The calculation of $n_c$ becomes impossible only at the lowest temperatures where the Hall coefficient becomes constant or as in sample 1C, 2C and 3C for which R increases after reaching a minimum as T is lowered. Fig. 3 shows the temperature dependence of $n = 1/Re$, $n_c$ and $n_i = n_o - n_c$ which are calculated by this model for samples 4 and 2c. R and n, at room temperature were considered as $R_{exh}$ and $n_o$ respectively. The curves show the typical behavior of the n, $n_c$ and $n_i$ for two simultaneous conduction processes.

We now turn to the problem of determining the compensation ratio of the melt-grown crystals. Analysis of the temperature dependence of the Fermi level $E_F$ provides a method for the simultaneous determination of the impurity activation energy $E_1$, the donors concentration $N_D$ and the compensation ratio $K = N_A/N_D$. If we assume that the number of impurity levels is equal to $2N_D$ due to the lifting of the spin degeneracy and if the distribution of the impurity levels is narrow, then[20]

$$n_i = \frac{2N_D}{1 + \exp[(-E_1 - E_F)/kT]} \qquad (18)$$

Hence,

$$E_F = -E_1 - kT\ln\left(\frac{2N_D}{n_o - n_c} - 1\right) \qquad (19)$$

When $n_c \ll n_o$, the temperature region below the temperature of the Hall-coefficient maximum, the temperature dependence of $E_F$ is a straight-line which intersects the ordinate at the point $E_F = -E_1$ and whose slope $-\ln[2N_D/(n_o-n_c)-1] \simeq -\ln[(1+K)/(1-K)]$ is determined by the degree of compensation $K = N_A/N_D$.

Knowing $n_c$ at any temperature, $E_F$ can be determined from the usual formula for a parabolic conduction band.

$$n_c = N_c F_{1/2}(\tilde{E}_F) \qquad (20)$$

where the functions $F_{1/2}(\tilde{E}_F)$ are tabulated Fermi integrals[28], $\tilde{E}_F = E_F/kT$ and $N_c$ is the effective conduction band density of states. Fig. 4 gives the temperature dependence of $E_F$; for $N_D < 1.7\times10^{17}$ the dependence of $E_F$ on T is linear with zero or negative slope which is the characteristic of a narrow impurity band[26]. $E_1$, $N_D$, and K which were determined from the intercepts and the slopes of the lines in Fig. 4 are listed in Table V.

It is evident from this table that the activation energy $E_1$ decreases with increasing $N_D$. A comparison of different samples shows that $E_1$ depends not only on $N_D$, but also on $N_A$ or K. The last row in Table V shows that the compensation in Cr- doped samples is very large and unfortunately the density of acceptors is varying from sample to sample. Hence it is difficult to do a systematic and quantitative study of transmutation doping in Cr- doped samples. The analysis of $E_F$ is based on the assumption that the impurity band is narrow and separated from the conduction band. As is discussed by H. Fritzsche[29], this assumption gets to a serious problem at carrier concentration above the M-NM transition density $N_c$. All our melt-grown samples have carrier densities near or above $N_c$, therefore one should not take the number listed in Table V too seriously.

### C. Expitaxial sample

The thermal neutron fluence for this sample was $7.5\times10^{15}$ n/cm$^2$ which

corresponds to an expected $n_{NTD} = 1.27 \times 10^{15} cm^{-3}$. Figure. 5 shows the temperature dependence of R and $\rho$ for the epitaxial sample. R has a maximum at about 4.2K; the slope of $\rho$ changes at about the same temperature. This again is the transition temperature between dominant band conduction at higher temperatures and impurity conduction at lower temperatures. At low temperatures this sample has an activated resistivity. For phonon assisted hopping between donor sites we can write[25]

$$\rho = \rho_3 \exp(E_3/kT) \tag{21}$$

Calculated values of $\rho_3$ and $E_3$ from the experimental curve are given in Table VI. These values are close to the reported values for samples similar to ours by Halbo and Sladek[30] and by Kahlert and Landwehr[31].

Fig. 6 gives the temperature dependence of n = 1/Re for the epitaxial sample. The curve was obtained by fitting the measured carrier concentration to the following expression

$$\frac{n(N_A + n)}{(N_D - N_A - n)} = \frac{N_c}{2} \exp\ (E_D/kT) \tag{22}$$

$E_D$ is the ionization energy of the donor impurities. The values of $N_D$, $N_A$, and $E_D$ which give the best fit are listed in Table VI. Deviation of the data from the calculated curve at low temperatures is due to the transition from band conduction to impurity conduction. The small dip in measured carrier concentration between 77 and 300K is caused by the temperature dependence of the Hall factor r, for polar optical phonon scattering[32].

Fig. 7 shows the temperature dependence of Hall mobility $\mu_H$ of the epitaxial sample. The sharp decrease below 6K is again due to the transition from band conduction to impurity conduction. The mobility curve was calculated by using a combination of scattering by polar optical phonons, piezoelectric acoustic phonons, deformation potential acoustic phonons, ionized impurities and neutral

impurities in the relaxation time[33]. At the temperatures between 6 and 60K the dominant scattering processes are those from ionized impurities and neutral impurities. Between 60 and 90K scattering by piezoelectric and acoustic phonons have some effect on the mobility; and at temperatures above 90K the dominant process is polar optical phonon scattering. The method of analysing polar optical phonon scattering failed completely between about 120 to 300K[33]. Because of this the calculated mobility was not extended above 120K. The values of $N_D$ and $N_A$ which best fit the experimental data are also given in Table VI. These values are somewhat larger than those obtained by analysing the temperature dependence of carrier density. However, the value of $N_D$-$N_A$ is the same. This indicates that there are some deep donor and acceptor centers which act as ionized impurity centers for scattering but do not contribute to the carrier density.

On the other hand the values of $N_D$ and $N_A$ which were calculated by using the Wolf master curve[34] of the mobility at 77K and which were reported by us earlier[8], were too large. This is because Wolfe's method does not include the effect of the deep impurities on the mobility.

## D. Magnetoresistance

Fig. 8 shows the field dependence of the magnetoresistance $\Delta\rho/\rho$ at 4.2K and 2.5K for some of the samples listed in Table III and IV. At low temperatures $\Delta\rho/\rho$ of all samples is negative up to the highest magnetic field used. The magnitude of $\Delta\rho/\rho$ increases with decreasing temperature. Following Zavaritskaya et al.[35] we assume that the magnetoresistance may be decomposed in two components

$$\Delta\rho/\rho = (\Delta\rho/\rho)_- + (\Delta\rho/\rho)_+ \qquad (23)$$

where the second term is the usual magnetoresistance due to the difference in the Lorentz forces for carriers with different velocities. It is proportional to $B^2$. The first term $(\Delta\rho/\rho)_-$ is believed to be due to the localized spin

alignment in the magnetic field and can be written as follows[30,35]

$$(\Delta\rho/\rho)_{-} \sim -(B/T+\theta)^2 \qquad B \to 0 \qquad (24)$$

$$(\Delta\rho/\rho)_{-} \to \text{constant} \qquad B \to \infty \qquad (25)$$

Thus for low magnetic field we have

$$\Delta\rho/\rho = -(B/T+\theta)^2 + bB^2 \qquad (26)$$

where b and $\theta$ are constants, which have different values for each sample. The values of $\theta$ and b which were deduced from the data of samples 1C and 3C using Eq.(26) are listed in Table VII. These values of $\theta$ and b are about three times larger than those reported by Halbo and Sladek[30] for their samples, which have a donor concentration of about a factor of 10 smaller than our samples.

The epitaxial sample with carrier concentration about $8.2\times10^{14}cm^{-3}$ at 300K has a positive magnetoresistance in the whole temperature range investigated as shown in Fig. 9. At high T in the band conduction range the field dependence of $\Delta\rho/\rho$ is quadratic at low fields and becomes close to linear at high field. In the impurity conduction range at low T the magnetoresistance is proportional to $B^2$. According to the theory of the weak field magnetoresistance for impurity conduction which was modified by Shklovskii[36] to include the results of percolation theory, the magnetic field dependence of the resistivity can be written as

$$\rho(B) = \rho\,(o)\,\exp\,(ta^{*}B^2e^2/N_Dc^2\hbar^2) \qquad (27)$$

where a* is the effective Bohr radius of impurity atoms and t is a constant. This theory predicts that the logarithmic derivative of $\rho(B)$ with respect to $B^2$ is independent of temperature. Our data shown in Fig. 10 is in good agreement with this prediction. We obtain t = 0.039 which is very close to the theoretical value[37] t = 0.04.

Fig. 11 shows the temperature dependence of magnetoresistance at 5kG.

Starting at high temperature, the magnetoresistance increases with decreasing temperature reaches a maximum at about 50K, and then decreases. This temperature dependence is very similar to that of the mobility (Fig.7). This is expected since for band conduction $\Delta\rho/\rho$ is a function of $(\mu B)$. The second maximum occurs at about 4.2K where the Hall coefficient has a maximum due to the transition from band conduction to impurity conduction. In the transition region the excess electron $n_o$ are divided into two parts, one part in the conduction band with one average velocity, the other part in the impurity band with different average velocity. In a magnetic field this velocity difference causes a magnetoresistance which is in addition to the magnetoresistance for two bands. This magnetoresistance which is important in the transition region can be written as follows[38]

$$\frac{\Delta\rho}{\rho o} = (\mu_i B)^2 \left[\frac{\sigma_c + \sigma_i b^2}{\sigma_c + \sigma_i} - \left(\frac{\sigma_c + \sigma_i b}{\sigma_c + \sigma_i}\right)^2\right] \qquad (28)$$

This equation reaches a maximum when $\sigma_c = \sigma_i$ which is the same condition as for the maximum of the Hall coefficient. The solid curve in Fig. 11 was computed by assuming that above 10K, $\Delta\rho/\rho$ is due to the band conduction only, below 3K, $\Delta\rho/\rho$ is solely due to the impurity conduction and a linear transition in between, and by adding to this magnetoresistance $\Delta\rho/\rho$ of the Eq. (28).

## VII. MAGNETORESISTANCE NEAR THE METAL-NONMETAL TRANSITION

The magnetoresistance of GaAs measured at 5kG and 4.2K is plotted against the room temperature carrier density in Fig. 12. Besides our own data we included the results of several other authors. As discussed in the previous section the large positive $\Delta\rho/\rho$ at small n is due to the shrinkage of the donor wavefunctions perpendicular to B. According to Eq. (27) this effect decreases

with increasing $N_D$ and hence with n. The observed decrease is however more rapid than expected from Eq. (27) because this equation ceases to be valid as the overlap of the donor wavefunctions becomes stronger. The magnetoresistance becomes negative for $n > 1.5 \times 10^{15} cm^{-3}$. The magnitude of this nagative $\Delta\rho/\rho$ reaches a maximum near $n = 10^{16} cm^{-3}$ and then decreases as n is increased to $10^{18} cm^{-3}$. This negative magnetoresistance is attributed to an interaction of free or semi-free carriers in the impurity band with magnetic moments of localized spins[35,39]. We conclude from Fig. 12 that the formation of the impurity band begins near $n = 2 \times 10^{15} cm^{-3}$ and that it has essentially merged with the conduction band near $5 \times 10^{17} cm^{-3}$.

According to Mott's criterion[40] the metal-nonmetal transition occurs at a critical concentration $N_c$ of the majority impurities

$$N_c = 0.018/(a^*)^3 \qquad (29)$$

independent of compensation. This yields $N_c = 2.3 \times 10^{16} cm^{-3}$ with $a^* = 92$ Å for n-type GaAs. In the following we compare our observations with Mott's criterion and the concentration of the maximum of the negative megnetoresistance with a model of Shmatrsev[39]. He has shown that the formation of localized spins requires fluctuations on a scale $r_1 > a_B, r_D$, meaning that if an impurity center is separated from its nearest neighbors by a distance $r > r_1$, the electron in that center will be localized; in this model it is assumed that the impurities are distributed randomly in accordance with the Poisson equation. With this assumption the density of localized magnetic moments, i.e., localized spins is

$$N_m = N \exp\left(-\frac{4}{3} \pi N r_1^3\right) \qquad (30)$$

where N is the total density of the impurities which is equal to electron concentration for non-compensated material. $N_m$ is maximum when $(4/3)\pi N r_1^3$ is equal to one. From Fig. 12 we see that the maximum of negative magnetoresistance occurs when the carrier concentration lies between $1 \times 10^{16} cm^{-3}$ and $2 \times 10^{16} cm^{-3}$

which for undoped GaAs gives

$$r_1 = (228\text{-}288)\ \mathring{A} \tag{31}$$

or

$$r_1 = (2\text{-}3)\ a^* \tag{32}$$

This value is the same as the value which was assumed in Ref. 39 for this model. For N larger than $N_{max}$, it seems that some clusters are formed because the decrease in negative magnetoresistance is slower than the exponential decrease of $N_m$. A similar curve for the negative magnetoresistance of Ge is given in Ref. 39 .

The M-NM transition occurs at impurity concentration at which the Hall coefficient and resistivity at low temperatures become independent of temperature[29]. From Fig. 1 and 2 we see that for undoped and n-type samples, the M-NM transition occurs at a concentration between $3.3\times10^{16}cm^{-3}$ (sample 0) and $4.7\times10^{16}cm^{-3}$ (sample 1) which corresponds with $K \simeq 0.3$ to $N_c=(5.7\pm0.7)\times10^{16}cm^{-3}$. This concentration is higher than $N_c = 2.3\times10^{16}cm^{-3}$ which we obtain from Mott's criterion[40].

As is shown by Fritzsche[41] and our data agrees (compare the curves for sample 3 and 3C in Fig. 2) with it, the M-NM transition shifts to higher carrier and majority impurity concentration with increasing degree of compensation. This is the cause of the observed shift of the M-NM transition of our undoped samples to a concentration higher than $N_c = 2.3\times10^{16}cm^{-3}$, since these samples contain an appreciable degree of compensation (see Table V). As mentioned earlier in this section, the maximum of negative magnetoresistance occurs at a carrier concentration between $1\times10^{16}cm^{-3}$ and $2\times10^{16}cm^{-3}$. This is close to the concentration corresponding to M-NM transition in undoped n-type GaAs. Hence it seems that these two phenomena are related. Since the critical concentration $N_c$ increases with compensation, one might be able to do a systematic study of the effect of compensation on the position of the maximum of the negative magnetoresistance

and see whether these two phenomena are indeed related.

Fig. 13 shows the carrier density dependence of the carrier mobilities at 300K in conduction band and of the Hall mobility of impurity conduction at 4.2K on the electron concentration at 300K. It appears that the mobilities extrapolate to the same value near $n = 5 \times 10^{17} cm^{-3}$. Above this concentration we believe the impurity band has merged with the conduction band. The decrease of the activation energies of undoped samples (see Table V) with increasing carrier concentration gives a similar indication. The peak of Hall coefficient in Fig. 2 is shrinking as the carrier density increases and becomes very small for sample #5 which has carrier density of about $3.7 \times 10^{17} cm^{-3}$. This shows that $b = \mu_c/\mu_i$ is decreasing to unity (see Eq.(17)) as carrier density increases and becomes close to one for sample #5. This is again an indication that the bands merge at a carrier density near $n = 5 \times 10^{17} cm^{-3}$. So we expect that the true metallic state in n-type GaAs starts at carrier density of about $5 \times 10^{17} cm^{-3}$. However, the presence of a small negative magnetoresistance above $n = 5 \times 10^{17} cm^{-3}$ suggests that some localized spins are still present in this true metallic region. This may be caused by some regions having a lower impurity concentration as a result of the random impurity distribution.

## VIII. SUMMARY AND CONCLUSIONS

Neutron transmutation doping is a well controlled and reproducible method for introducing shallow donors into GaAs crystals. This doping method is approximately 1000 times more efficient in GaAs than in Si because of the higher abundances and neutron capture cross sections of transmutable isotopes in GaAs. Moreover, the longest halflife encountered in the nuclear reactions in GaAs is only 26h compared to 14.3d in Si. Hence the induced radioactivity decays to an

acceptable low level for handling in a shorter time in GaAs than in Si. In epitaxially grown GaAs of high purity the recoil and radiation damage associated with transmutation doping can be removed by annealing at about 600°C which is below the critical temperature for As effusion. Hence no $Si_3N_4$ encapsulation is needed. In contrast, annealing near 800°C is required to remove the damage associated with doping by ion-implantation.

We found that such high annealing temperatures are also needed after transmutation doping of melt-grown GaAs crystals which were initially undoped or Cr-doped. In contrast to epitaxially grown GaAs, these crystals contain a high concentration of impurities and defects which can trap and bind either the transmuted atoms or the radiation (and recoil) defects and thus give cause for the higher annealing temperature.

After annealing we find that most transmuted Ge atoms are on Ga sites and most transmuted Se atoms are on As sites giving rise to shallow donors. The measured concentrations of added donors for various neutron fluences agrees well with the values deduced from the known abundances and neutron capture cross sections of the transmutable isotopes. Our data on Cr-doped samples are less conclusive in this respect because they contained a high degree of compensation which prevented a reliable determination of the donor concentration added by transmutation doping.

For the epitaxial GaAs sample the donor and acceptor concentrations $N_D$ and $N_A$ could be determined by two independent methods. The analysis of the temperature dependence of the carrier concentration n in the conduction band yielded $N_D$ and $N_A$ values which were somewhat smaller than the values obtained by analysing the temperature dependence of the mobility. We believe that the $N_D$ and $N_A$ values obtained from the T-dependence of n represent the concentration of shallow donors and acceptors which are relevant for comparison with the transmutation doping theory. The additional ionized impurities revealed by the mobility

analysis are most likely deep lying impurity or defect centers which do not affect the temperature dependence of the carrier concentrations.

The transmutation-doped epitaxial GaAs sample was nonmetallic and showed a transition from band conduction above 4.2K to impurity conduction below 4.2K. Its magnetoresistance $\Delta\rho/\rho$ was positive at all temperatures. The value of $\Delta\rho/\rho$ peaked at 50K, which corresponds to the temperature of maximum electron mobility in the conduction band, as well as at 4.2K where band conduction and impurity conduction have equal magnitude. Below 4.2K the magnetic field dependence of the resistivity agrees well with the theory of impurity conduction as modified by Shklovskii[36,37].

After transmutation doping our undoped as well as some of our Cr-doped melt-grown GaAs crystals were metallic, which means, that R and $\rho$ were temperature independent at the lowest temperatures. The magnetoresistance of the melt-grown samples was negative at low temperatures and increased in magnitude with decreasing temperature. This is in accordance with the theory of scattering of charge carriers from localized spins partially aligned in the magnetic field[42].

A compilation of data from various authors and obtained by us revealed that the low temperature magnetoresistance changes from positive to negative as the room temperature carrier concentration $n_o$ is increased. The transition occurs near $n_o = 2\times10^{15}cm^{-3}$ which is on the nonmetallic side of the nonmetal-metal transition. The negative magnetoresistance reaches a maximum value near $n_o = 10^{16}cm^{-3}$ and then decreases with increasing $n_o$. It disappears when $n_o$ approaches $5\times10^{17}cm^{-3}$ which is the range of the so-called true metallic state which is characterized by the absence of a Hall effect maximum at higher temperatures.

We found that the nonmetal-metal transition occurs near $N_c = 5.7\times10^{16}cm^{-3}$ which is higher than the critical concentration $N_c = 2.3\times10^{16}cm^{-3}$ calculated

from Mott's criterion[40] for this transition. We attribute this observation to the fact that our samples contain an appreciable degree of compensation. On the basis of physical arguments as well as experimental evidence Fritzsche[41] pointed out that the critical concentration $N_c$ increases with compensation.

Our observation that the maximum of the negative magnetoresistance and the nonmetal-metal transition occur at close carrier concentrations $n_o$ suggests that these two phenomena are related.

In summary, we find that transmutation doping is a convenient method of introducing a desired concentration of shallow donors into GaAs crystals for modifying their electronic properties.

## IX. REFERENCES


1. J. W. Cleland, K. Lark-Horovitz and C. Pigg, Phys. Rev. 78, 814 (1950).
2. H. Fritzsche and M. Cuevas, Phys. Rev. 119, 1238 (1960).
3. M. Cuevas, Phys. Rev. 164, 1021 (1967).
4. S. Golin, Phys. Rev. 132, 178 (1963).
5. A. Kuehnel, H. Siethoff and G. Landwehr, Phys. Status Solidi A29, 387 (1975).
6. F. Kuchar, E. Fantner and G. Bauer, Phys. Status Solidi A 24, 513 (1974).
7. Sh. M. Mirianashvili and D. I. Nanobashvili, Fiz. Tekh. Poluprovodn. 4, 1879 (1970) [Sov. Phys. Semicond. 4, 1612 (1971)].
8. M. A. Vesaghi and H. Fritzsche, Proceedings of 3rd Intl. Conf. on Neutron Transmutation Doped Silicon, Copenhagen, TOPSIL 1980.
9. R. Weast, Handbook of Chemistry and Physics, 58th ed. (CRC Press, Florida, 1977-1978) p B-282,B284.
10. Brookhaven National Laboratory 325 3rd ed. V1, National Neutron Cross Section Center (1973), p.B/69,B/70,B/78 .
11. L. W. Aukerman, P.W.Davis, R.D.Graft and T.S.Shilliday, J. Appl. Phys. 34, 3590 (1963).
12. Reactor Physics Constants, ANL-5800 2nd Ed. 631 (1963).
13. R. Bauerlein, Z. Nutarforsch, 14A, 1069 (1959); Z. Phys. 176, 498 (1963).
14. Kindly supplied to us by Prof. C. M. Wolfe of Washington University, St. Louis.
15. E. Munoz, W. L. Snyder and J. L. Moll Appl. Phys. Lett. 16, 262 (1970).
16. T.S. Blakmore, Solid State Physics 2nd Ed.,(W.B.Saunders, Philadelphia, 1974),p.340.
17. O. V. Emelanenko, T. S. Lagunova and D. N. Nasledov, Fiz. Tverd. Tela, 3, 198 (1961)[Sov. Phys. Solid State 3, 144 (1961)].
18. D. J. Oliver, Phys. Rev. 127, 1045 (1962).

19. J. F. Woods and C. Y. Chen, Phys. Rev. 135A, 1462 (1964).

20. O. V. Emelyanenko, T. S. Lagunova, D. N. Nasledov, and G. N. Talalakin, Fiz. Tverd. Tela 7, 1315 (1965) [Sov. Phys. Solid State 7,1063 (1965)].

21. O. V. Emelyanenko, D. N. Nasledov and N. A. Urmanov, Phys. Status Solidi 32, K175 (1969).

22. Kh. I. Amirkhanov, R. I. Bashirov and A. Yu. Mollaev, Fiz. Tverd. Tela 13, 849 (1971)[Sov. Phys. Solid State 13, 701 (1971)].

23. B. M. Vol., E. I. Zavaritskaya, I.D.Voronova and N. V. Rozhdestrenskaya, Fiz. Tekh. Poluprovodn. 5, 943 (1971) [Sov. Phys. Semicond. 5, 829 (1971)].

24. V. M. Guslikov, O. V. Emelyanenko, D. N. Nasledov, D. D. Nedeoglo and I. N. Timchenko, Fiz. Tekh. Poluprovodn. 7, 1785 (1973) [Sov. Phys. Semicond. 7, 1191 (1974)].

25. H. Fritzsche, J. Phys. Chem. Solids 6, 69 (1958).

26. R. J. Sladek, J. Phys. Chem. Solids 5, 157 (1958).

27. C. S. Hung, Phys. Rev. 79, 727 (1950).

28. A. C. Beer, M. N. Chase and P. F. Choquard, Helv. Phys. Acta 28, 529 (1955).

29. H. Fritzsche, in Proceedings of the 19th Scottish Universities Summer School in Physics 1978, edited by L. R. Friedman and D. P. Tunstall (SUSSP Publications, Department of Physics, University of Edinburgh, 1978), p 193..

30. L. Halbo and J. Sladek, Phys. Rev. 173, 794 (1968).

31. H. Kahlert and G. Landwehr, Z. Phys. B24, 361 (1976).

32. G. E. Stillman,C.M. Wolfe, and J. O. Dimmock, J. Phys. Chem. Solids 31, 1199 (1970).

33. C.M.Wolfe,G. E. Stillman and W. T. Lindley, J. Appl. Phys. 41, 3088 (1970). There are some printing mistakes in the equation of ionized impurity relaxation time of this publication, the correct form is

$$1/\tau_{II}\ (x) = 1.20763[(2N_A + n)/\varepsilon_o{}^2]\ (m^*/m)^{-1/2}T^{-3/2}g\ x^{-3/2}$$

34. C.M.Wolfe, G. E. Stillman and J. P. Dimmock, J. Appl. Phys. 41, 504 (1970).

35. E. I. Zavaritskaya,I. D. Voronova and N. V. Rozhdestvenskaya, Fiz. Tekh. Poluprovodn. 6, 1945 (1972) [Sov. Phys. Semicond. 6, 1668 (1973)].

36. B. I. Shklovskii, Fiz. Tekh. Poluprovodn. 6, 1197 (1972) [Sov. Phys. Semicond. 6, 1053 (1973).

37. B. I. Shklovskii, Fiz. Tekh. Poluprovodn. 8, 416 (1974) [Sov. Phys. Semicond. 8, 268 (1974)].

38. V. H. Schonwald, Z. Naturforsch, 19A, 1276 (1964).

39. Yu. V. Shmatrsev, E. F. Shender and T. A. Polyanskaya, Fiz. Tekh. Poluprovodn. 4, 2311 (1970) [Sov. Phys. Semicond. 4, 1990 (1971)].

40. N. F. Mott, Proc. Phys. Soc. (London) 62, 416 (1949); Phil. Mag. 6 287 (1961); Adv. Phys. 16, 49 (1967).

41. H. Fritzsche, Phil. Mag. B42, 835 (1980).

42. Toyozawa, J. Phys. Soc. Jpn. 17, 986 (1962).

Table I. Concentration, capture cross section and resonance integral for Ga and As isotopes.

| Isotops | n,($10^{22}cm^{-3}$) | $\sigma_c^i$(barn) | $I^i$(barn) |
|---|---|---|---|
| $^{69}Ga$ | 1.332 | $1.68\pm0.07$[a] | $15.6\pm1.5$[a] |
| $^{71}Ga$ | 0.881 | $4.86\pm0.28$[a] | $31.2\pm1.9$[a] |
| $^{75}As$ | 2.213 | $4.3\pm0.1$ [a] | $60\pm4$ [a] |

[a]Reference 10

Table II. Recoil energies in eV

| Isotope | $E_R(1\gamma)$ | $E_R(2\gamma)$ | $E_R(3\gamma)$ | $E_R(\beta_{max})$ | $E_R(\beta)$ |
|---|---|---|---|---|---|
| $^{70}Ga$ | 457 | 228 | 152 | 33 | 16 |
| $^{72}Ga$ | 444 | 222 | 148 | 100 | 50 |
| $^{76}As$ | 375 | 187 | 125 | 83 | 41 |

Table III. Characteristics at 300K of undoped GaAs samples before and after transmutation doping.

| | Sample No.: | 0 | 1 | 2 | 3 | 4 | 5 |
|---|---|---|---|---|---|---|---|
| Before irradiation | $R(cm^3/C)$ | 263 | 216 | 111 | 254 | 249 | 245 |
| | $\rho$(ohm-cm) | 0.07 | 0.06 | 0.029 | 0.072 | 0.07 | 0.068 |
| | $n(10^{16}cm^{-3})$ | 2.37 | 2.89 | 5.64 | 2.46 | 2.5 | 2.55 |
| | $\mu_H(10^3cm^2/Vs)$ | 3.78 | 3.6 | 3.8 | 3.53 | 3.56 | 3.6 |
| | $\Phi(10^{17}n/cm^2)$ | 0 | 1.0 | 1.0 | 2.0 | 9.37 | 18.75 |
| | anneal time(h) | 10.5 | 5 | 12.5 | 10.5 | 4.5 | 4.5 |
| After irradiation and annealing | $R(cm^3/C)$ | 193 | 131 | 78.9 | 101 | 37.5 | 19.2 |
| | $\rho$(ohm-cm) | 0.04 | 0.035 | 0.021 | 0.024 | 0.0094 | 0.0055 |
| | $n(10^{16}cm^{-3})$ | 3.23 | 4.75 | 7.91 | 6.2 | 16.7 | 32.5 |
| | $\mu_H(10^3cm^2/Vs)$ | 4.35 | 3.71 | 3.8 | 4.19 | 3.97 | 3.47 |
| | $\Delta n(10^{16}cm^{-3})$ | 0.86 | 1.86 | 2.27 | 3.74 | 14.2 | 30 |
| | $n_{NTD}(10^{16}cm^{-3})$ | 0 | $1.72\pm0.15$ | $1.72\pm0.15$ | $3.44\pm0.27$ | $16.1\pm1.4$ | $32.1\pm2.7$ |

Table IV. Characteristics at 300K of Cr-doped GaAs samples after transmutation doping.

| Sample No.: | 1C | 2C | 3C | 4C |
|---|---|---|---|---|
| $R(cm^3/C)$ | 560 | 323 | 111 | 40.2 |
| $\rho$(ohm-cm) | 0.235 | 0.143 | 0.043 | 0.014 |
| $\mu_H(10^3 cm^2/Vs)$ | 2.38 | 2.25 | 2.56 | 2.97 |
| $n(10^{16} cm^{-3})$ | 1.1 | 1.72 | 5.63 | 15.5 |
| $n_{NTD}(10^{16} cm^{-3})$ | $8.0 \pm 0.7$ | $9.65 \pm 0.8$ | $16.1 \pm 1.4$ | $32.2 \pm 2.7$ |

Table V. Activation energy $E_1$, donor concentration $N_D$ and compensation ratio K, calculated by using two band model.

| Sample No. : | 0 | 1 | 2 | 3 | 4 | 1C | 2C | 3C |
|---|---|---|---|---|---|---|---|---|
| $E_1$(mev) | 3.7 | 2.6 | 2.9 | 3 | 1.2 | 1.7 | 0.15 | 3.2 |
| $N_D(10^{16} cm^{-3})$ | 5 | 7 | 8 | 6.7 | 17.3 | 8.5 | 13 | 12.5 |
| $K=N_A/N_D$ | 0.3 | 0.3 | $\sim 0$ | 0.06 | $\sim 0$ | 0.87 | 0.85 | 0.52 |

Table VI. Characteristics of epitaxial sample

| $\rho_3$(ohm-cm) | $E_3$(mev) | $E_D$(mev) | $N_D(10^{14}cm^{-3})$ | $N_A(10^{14}cm^{-3})$ |
|---|---|---|---|---|
| | | | 8.6[a] | 0.2[a] |
| 4500 | 0.51 | 4.7a | | |
| | | | 9.8[b] | 1.4[b] |

[a]Analyzing T dependence of n

[b]Analyzing T dependence of $\mu_H$

Table VII. θ and b, were deduced from negative magnetoresistance data

| Sample No.: | 1C | 3C |
|---|---|---|
| θ(°K) | 5.5 | 5.8 |
| $b(10^{-3}kG^{-2})$ | 5.3 | 4.8 |

## FIGURE CAPTIONS

Fig. 1. Temperature dependence of the resistivity of GaAs samples. The characteristics of these samples are listed in Tables III and IV.

Fig. 2. Temperature dependence of the Hall coefficient of the samples of Fig. 1.

Fig. 3. Temperature dependence of n = 1/Re, concentration of carriers in conduction band $n_c$, concentration of carriers in the impurity band $n_i$, and carrier concentration at 300K, $n_o$ of samples 4 and 2C.

Fig. 4. Fermi energy as a function of absolute temperature of some of the samples listed in Table III and IV.

Fig. 5. Temperature dependence of the Hall coefficient and the resistivity of the epitaxial sample.

Fig. 6. Carrier concentration n as a function of 1/T of epitaxial sample. Solid surve is the best fit of Eq. (22) of text to the experimental data.

Fig. 7. Temperature dependence of the Hall mobility of the sample of Fig. 6. Solid curve is the calculated combined mobility (see text).

Fig. 8. Magnetic field dependence of the magnetoresistance of some of the samples listed in Tables III and IV at 4.2K and 2.5K.

Fig. 9. Magnetic field dependence of the magnetoresistance of the epitaxial sample at different temperatures.

Fig. 10. Resistivity as a function of the square of the magnetic field at temperatures below 4.2K of the sample of Fig. 9.

Fig. 11. Temperature dependence of the magnetoresistance at 5kG of the epitaxial sample. Solid curve is the magnetoresistance calculated by the method described at the end of section VI.

Fig. 12. Magnetoresistance at 5kG and 4.2K as a function of carrier concentration at 300K of our samples and those of other authors.

Fig. 13. Hall mobility as a function of the room temperature carrier density of the samples listed in Tables III and IV.

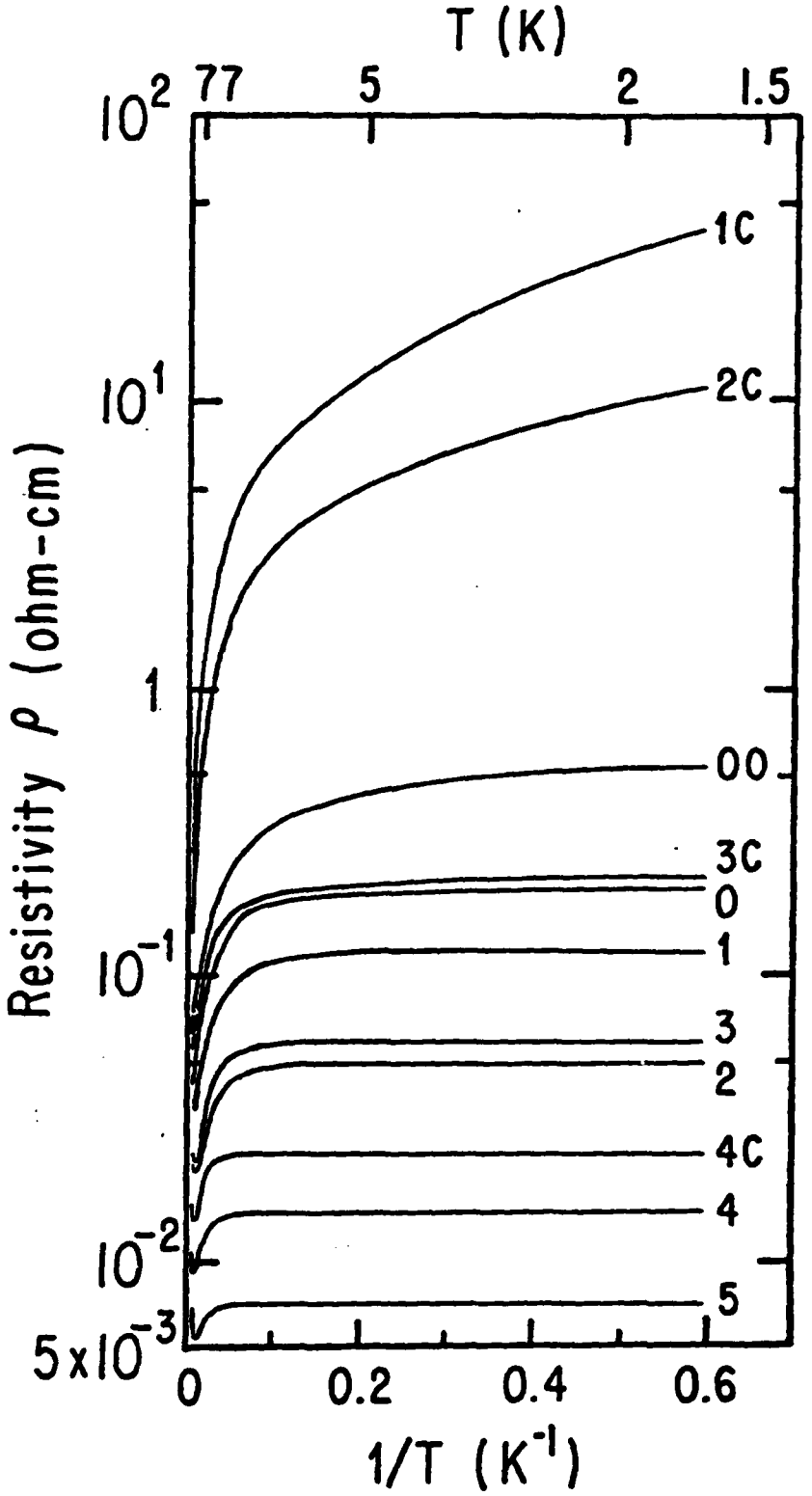
T (K)
77
5
2
1.5
$10^2$
$10^1$
1
$10^{-1}$
$10^{-2}$
$5\times10^{-3}$
Resistivity ρ (ohm-cm)
1C
2C
00
3C
0
1
3
2
4C
4
5
0
0.2
0.4
0.6
1/T ($K^{-1}$)

Fig. 1

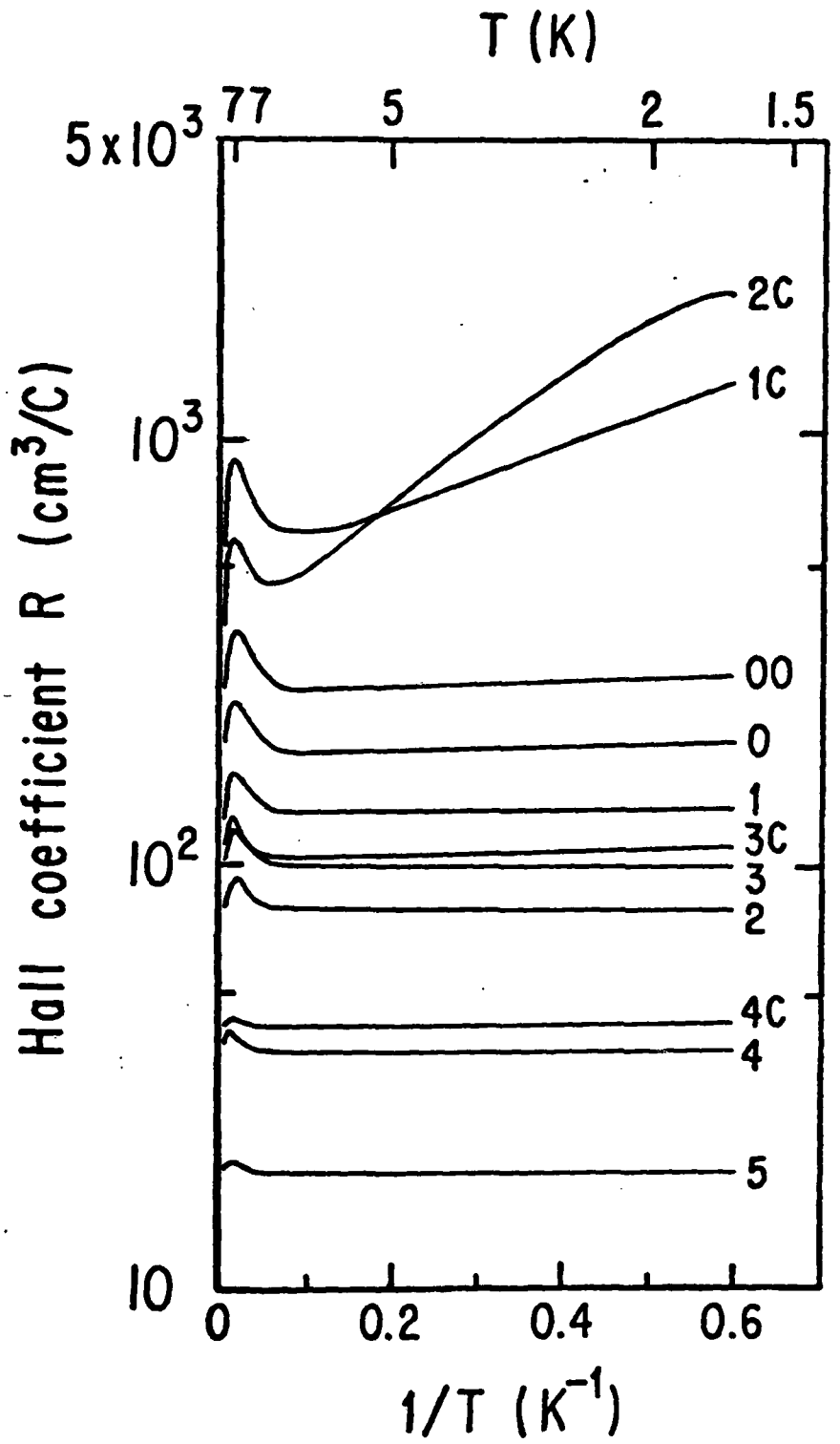
T (K)
77
5
2
1.5
5x10^3
10^3
10^2
10
Hall coefficient R (cm^3/C)
2C
1C
00
0
1
3C
3
2
4C
4
5
0
0.2
0.4
0.6
1/T (K^-1)

Fig. 2

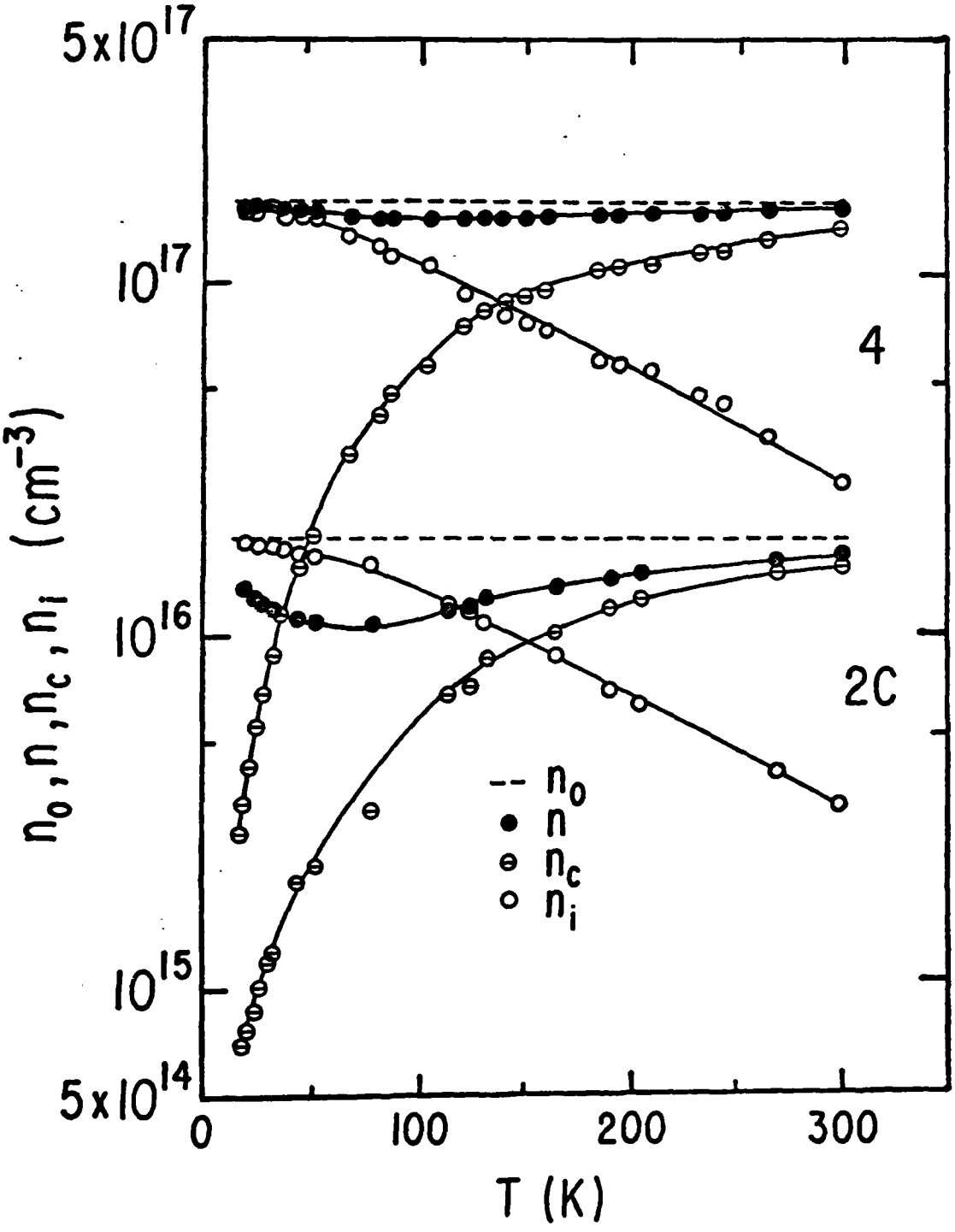
5x10^17
10^17
10^16
10^15
5x10^14
0
100
200
300
T (K)
n0, n, nc, ni (cm^-3)
4
2C
n0
n
nc
ni

Fig. 3

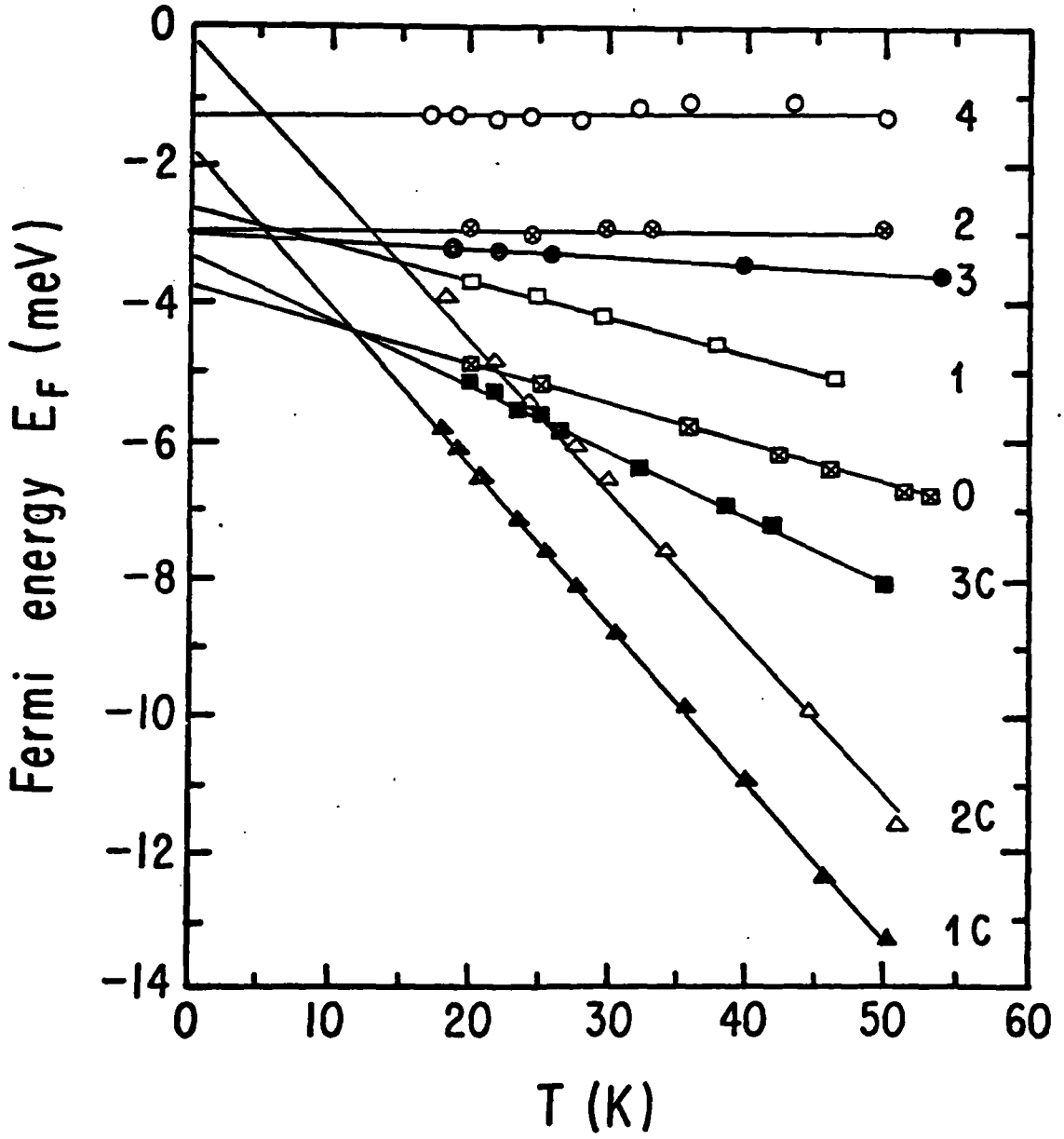
0
-2
-4
-6
-8
-10
-12
-14
Fermi energy $E_F$ (meV)
0
10
20
30
40
50
60
T (K)
4
2
3
1
0
3C
2C
1C

Fig. 4

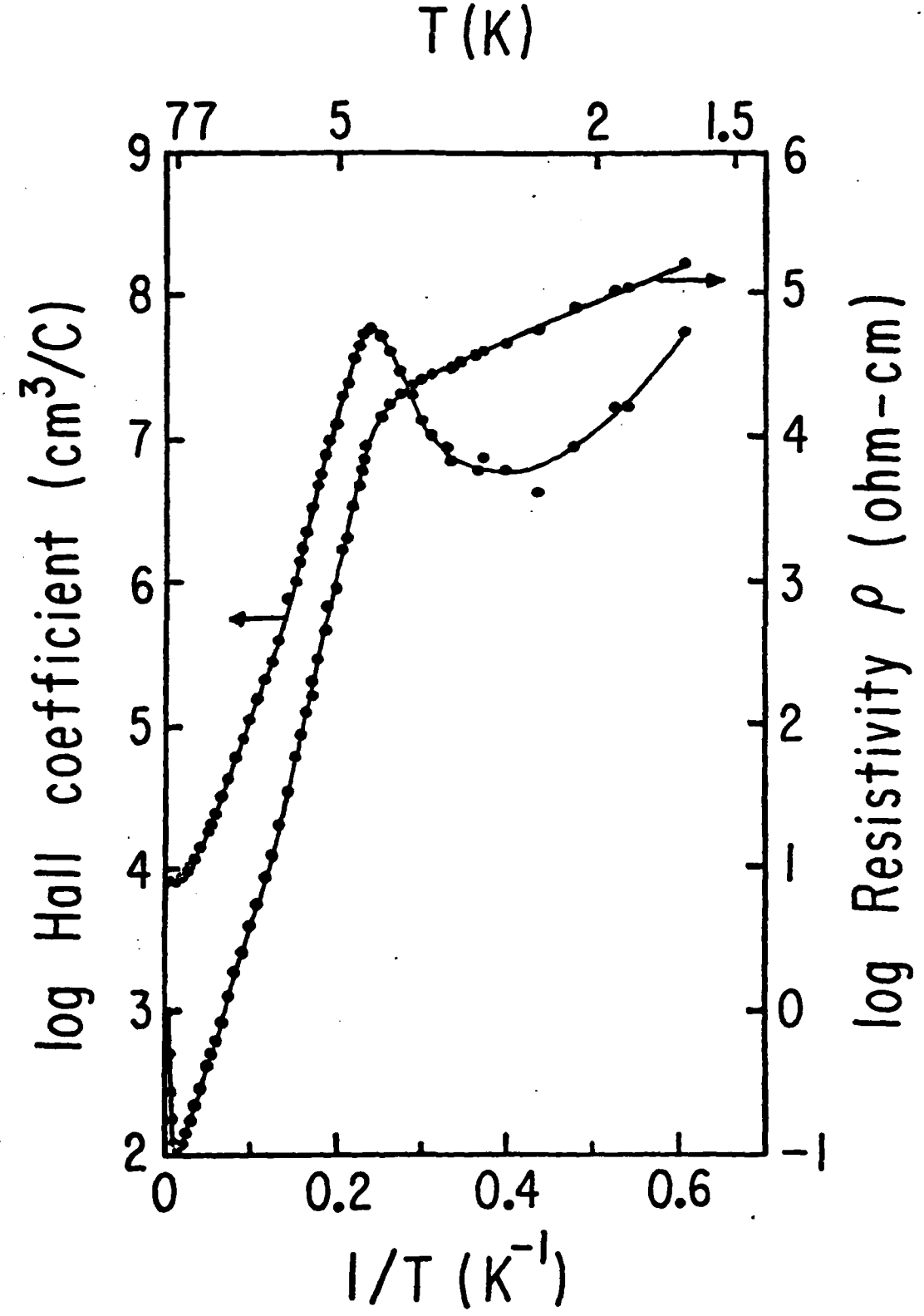
T(K)
77
5
2
1.5
9
8
7
6
5
4
3
2
0
0.2
0.4
0.6
1/T (K⁻¹)
log Hall coefficient (cm³/C)
6
5
4
3
2
1
0
-1
log Resistivity ρ (ohm-cm)

Fig. 5

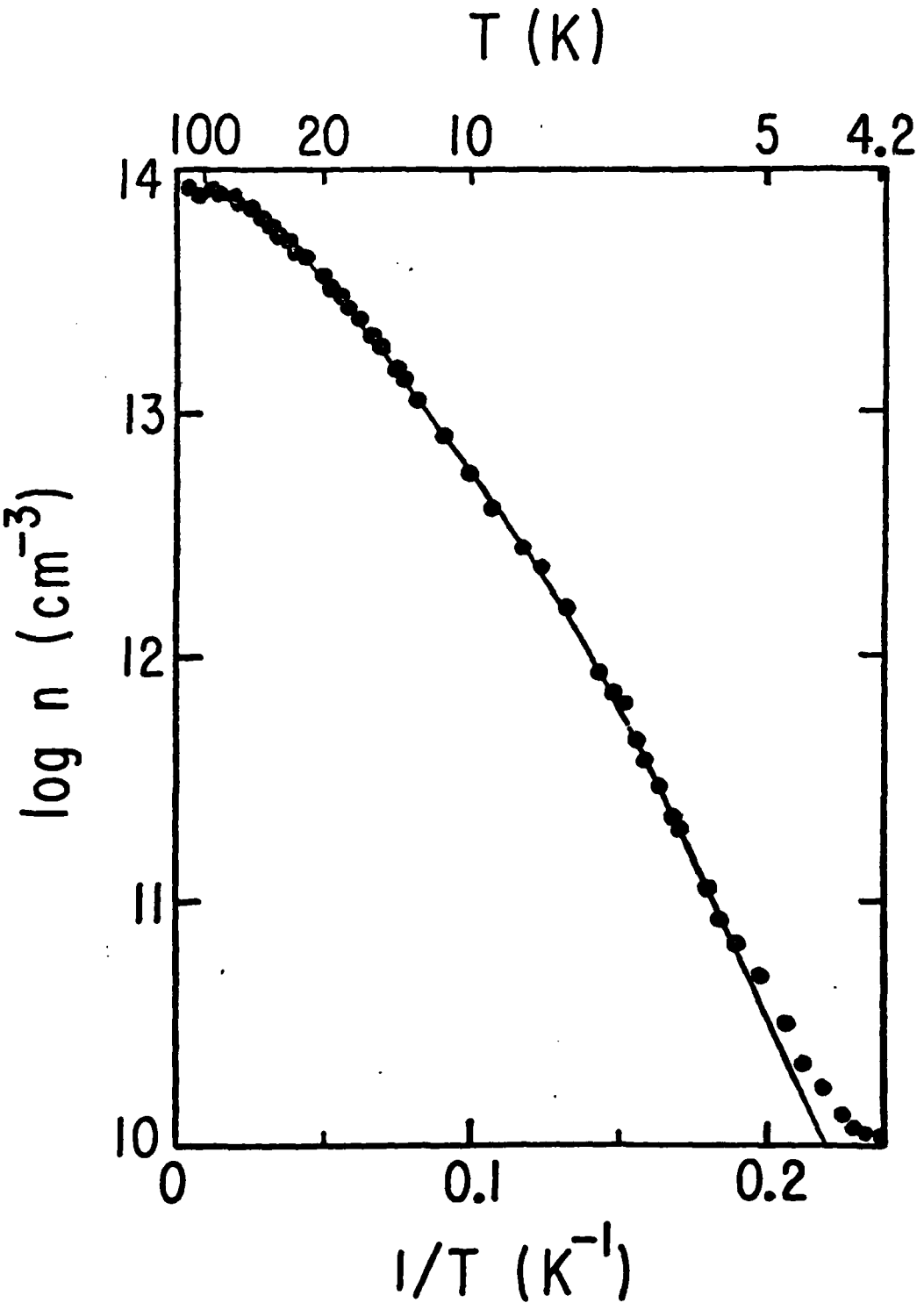


Fig. 6

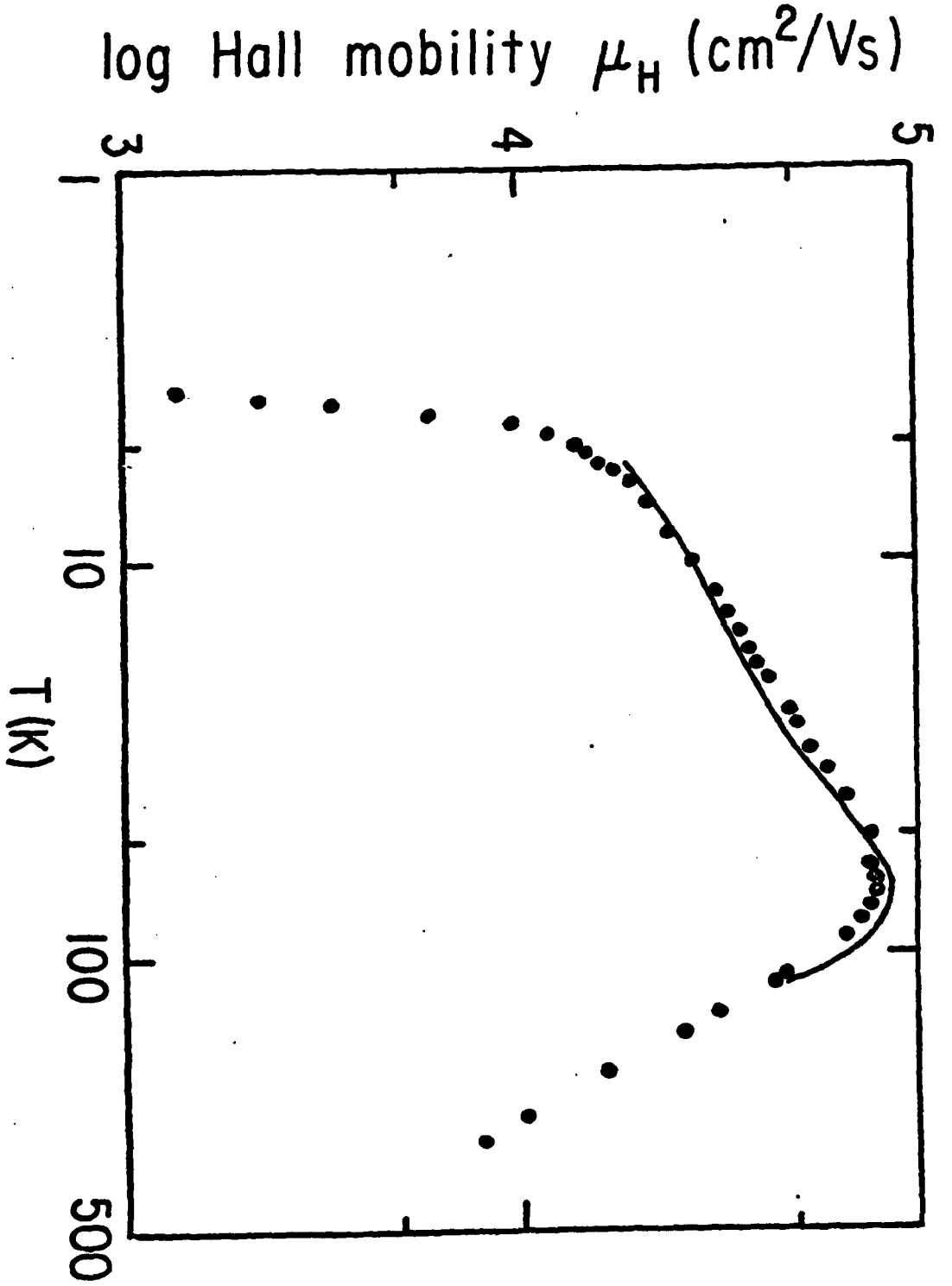


Fig. 7

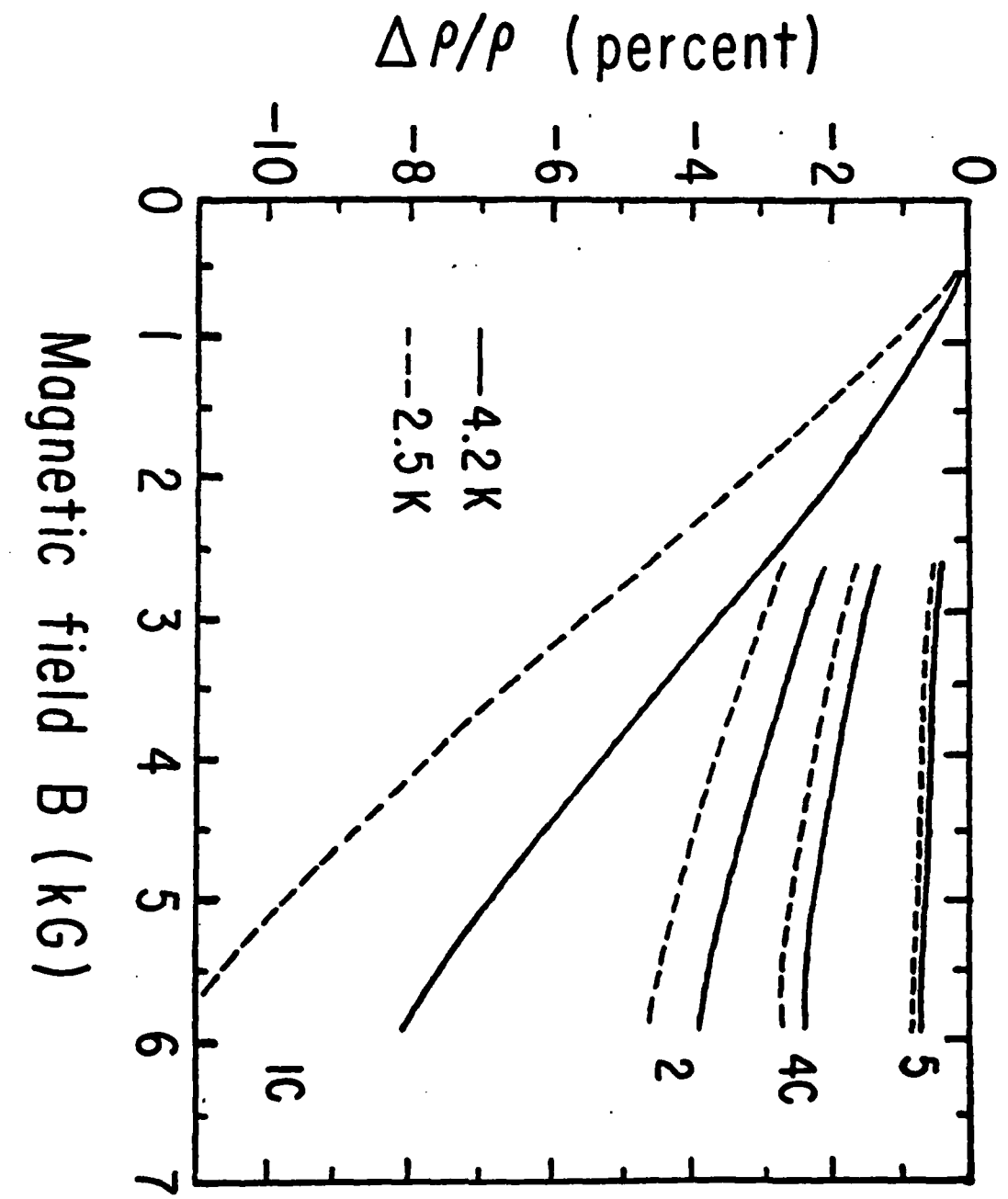
Δρ/ρ (percent)
−10
−8
−6
−4
−2
0
0
1
2
3
4
5
6
7
Magnetic field B (kG)
—4.2K
---2.5K
1C
2
4C
5

Fig. 8

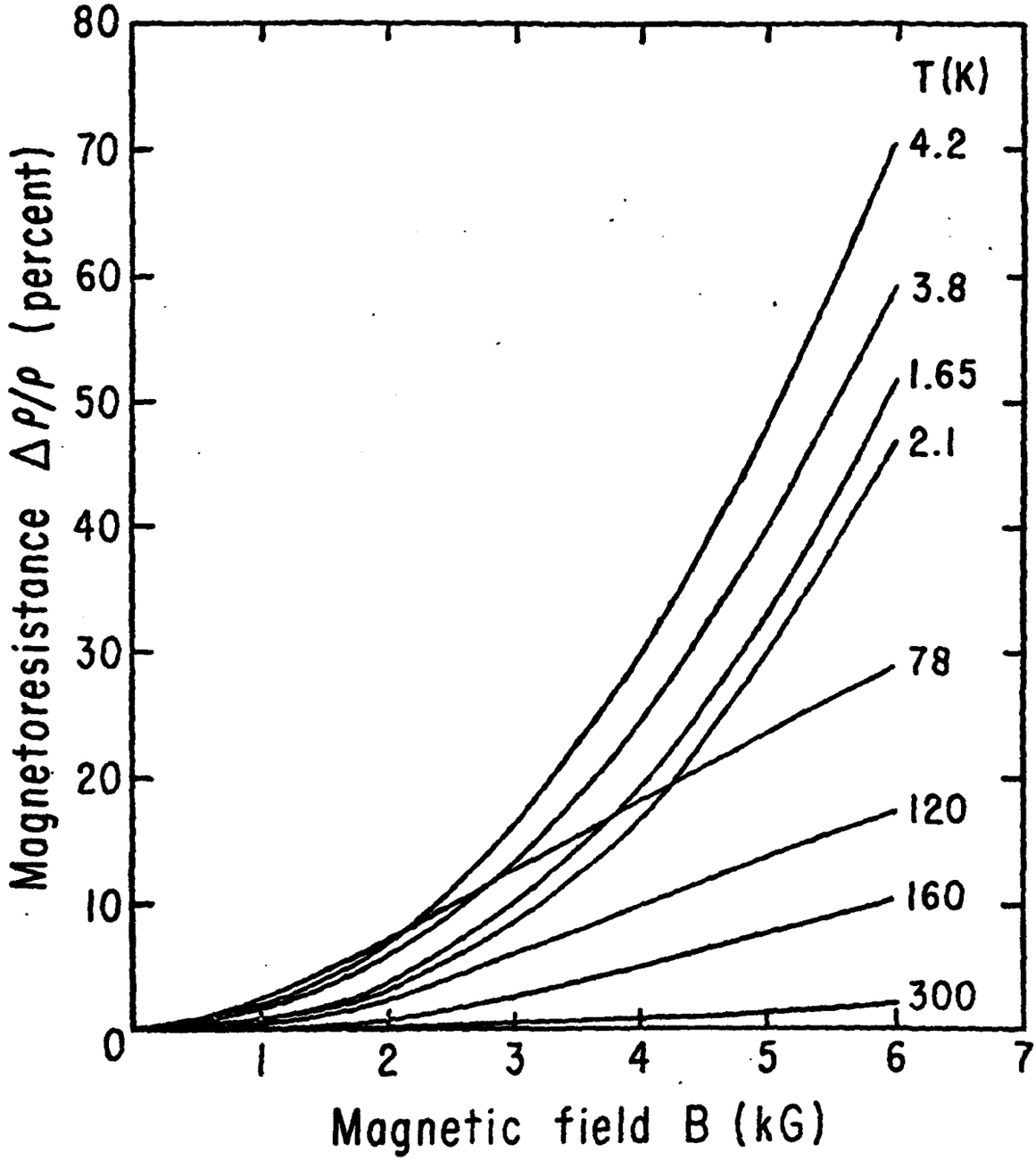
80
70
60
50
40
30
20
10
0
1
2
3
4
5
6
7
T(K)
4.2
3.8
1.65
2.1
78
120
160
300
Magnetoresistance Δρ/ρ (percent)
Magnetic field B (kG)

Fig. 9

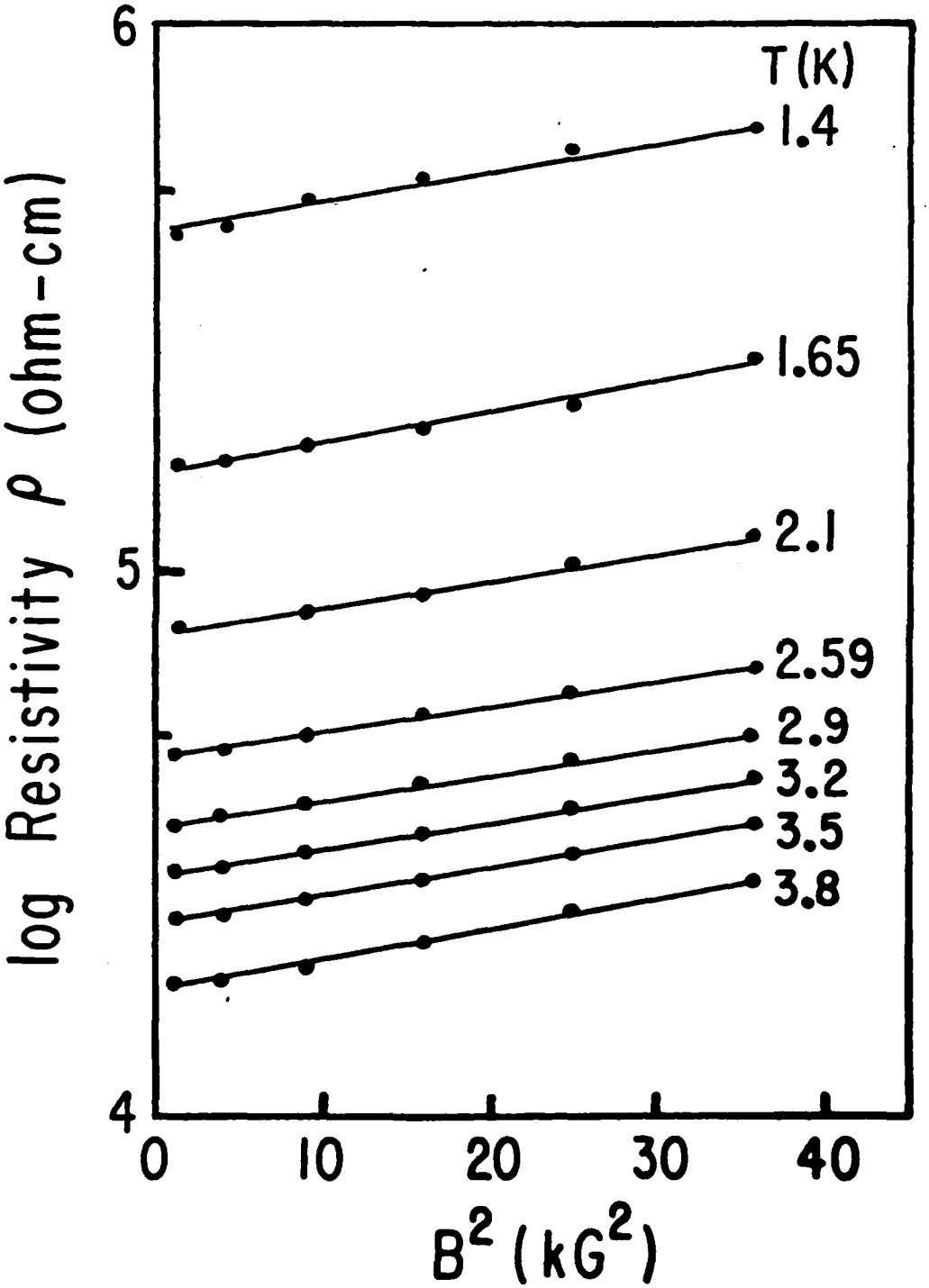
6
5
4
log Resistivity ρ (ohm-cm)
T(K)
1.4
1.65
2.1
2.59
2.9
3.2
3.5
3.8
0
10
20
30
40
B² (kG²)

Fig. 10

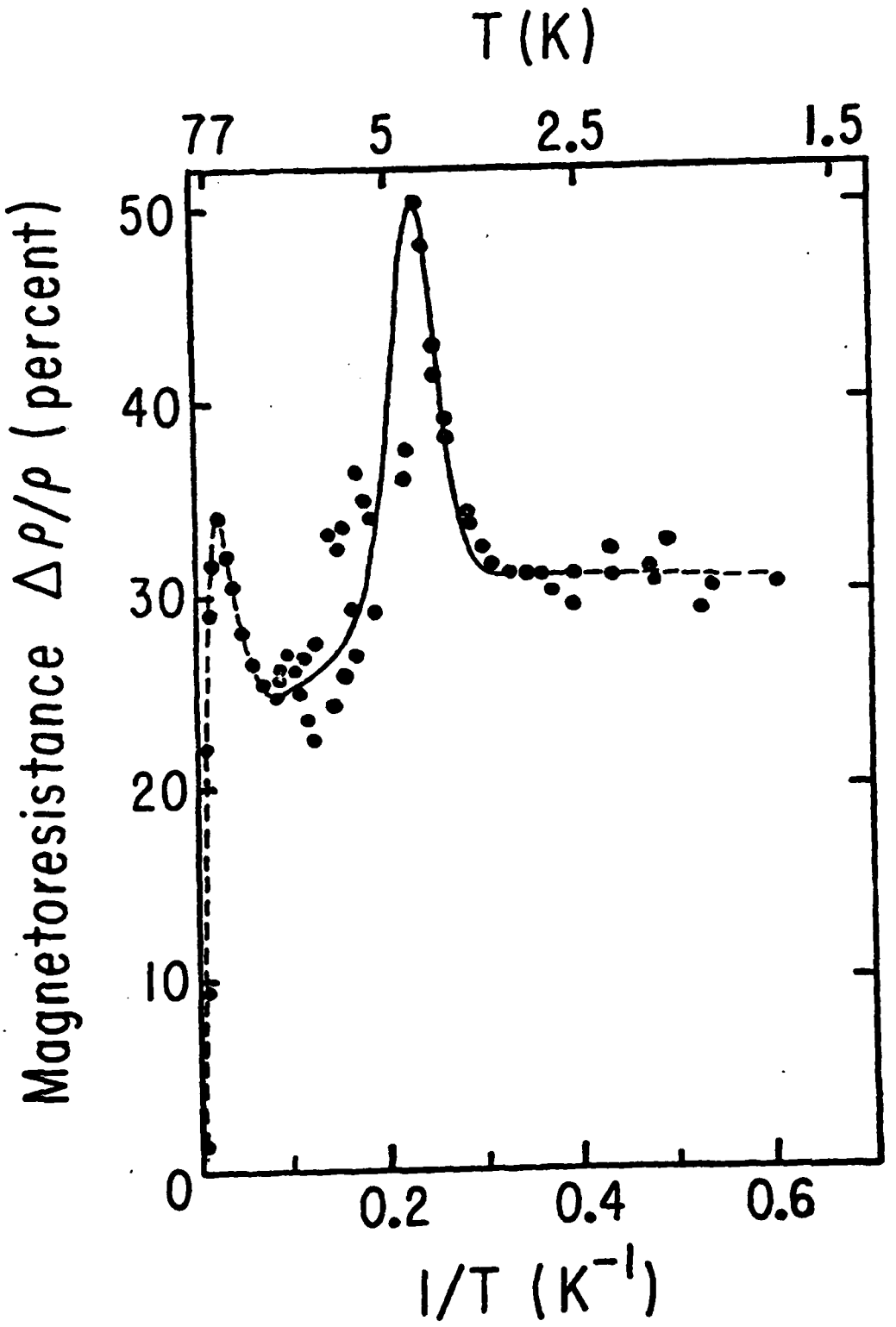
T (K)
77
5
2.5
1.5
Magnetoresistance Δρ/ρ (percent)
50
40
30
20
10
0
0.2
0.4
0.6
1/T (K⁻¹)

Fig. 11

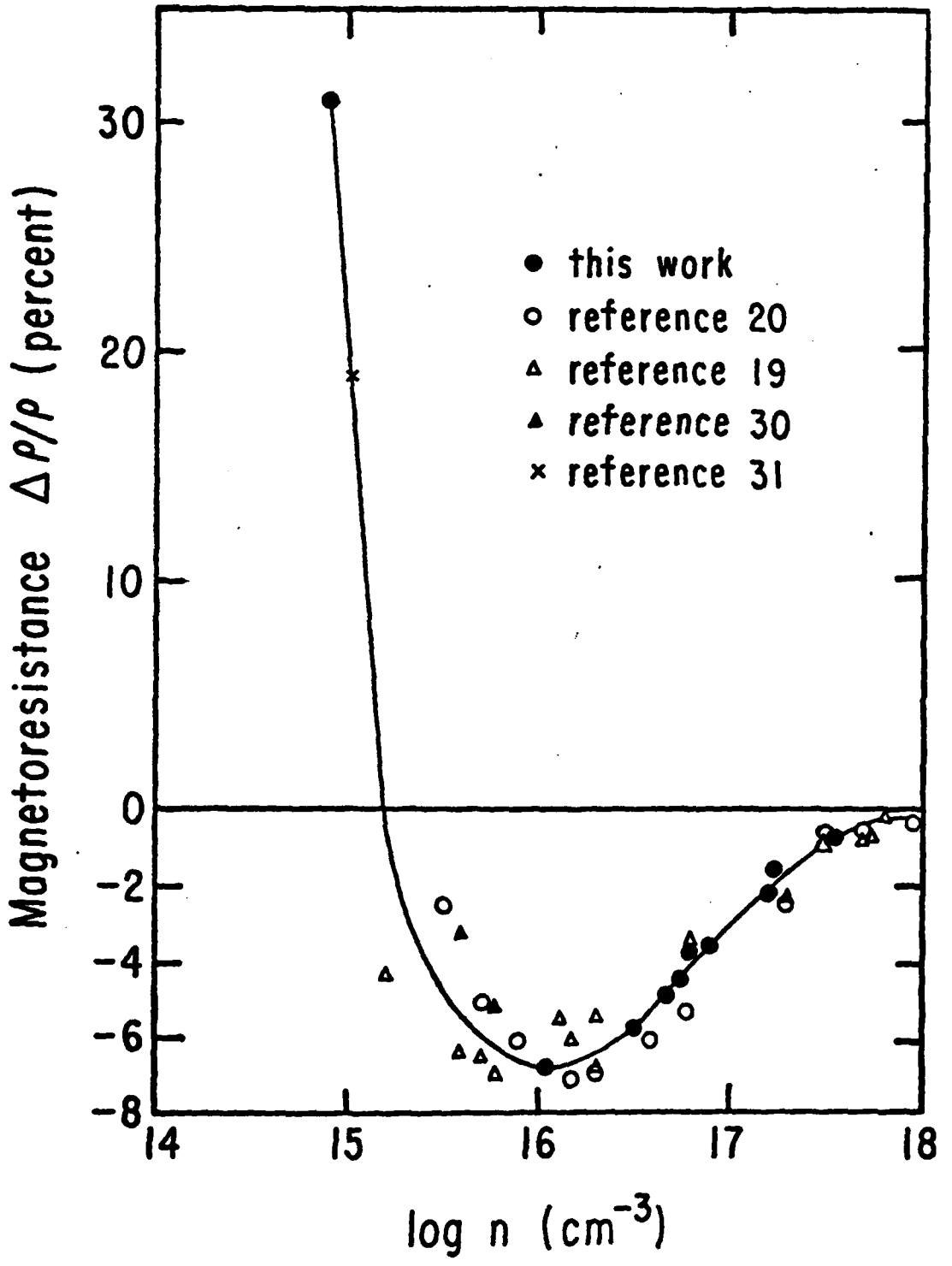
30
20
10
0
-2
-4
-6
-8
14
15
16
17
18
Magnetoresistance Δρ/ρ (percent)
log n (cm⁻³)
this work
reference 20
reference 19
reference 30
reference 31

Fig. 12

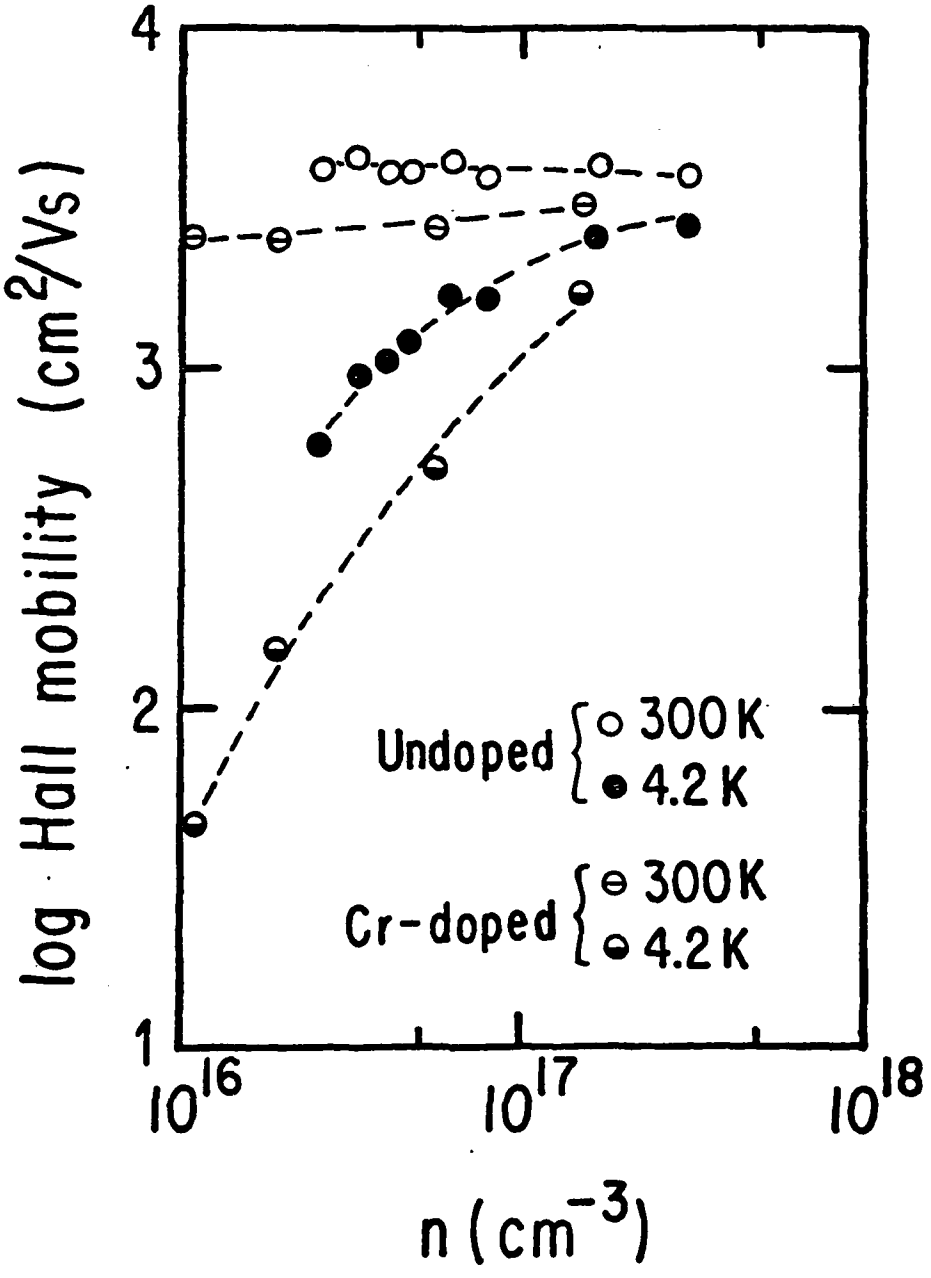
4
3
2
1
log Hall mobility (cm²/Vs)
Undoped
300 K
4.2 K
Cr-doped
300 K
4.2 K
10¹⁶
10¹⁷
10¹⁸
n (cm⁻³)

Fig. 13

# XIII. PUBLICATIONS

"Electrical Properties of Neutron Transmutation Doped GaAs Below 450K" by M.A. Vesaghi, Phys. Rev. B (in press).